Iron sand-based $Mn_{0.3}Fe_{2.7}O_4$ nanofluid as a new magnetic field sensor

Delianti[1,2], ST. Ulfawanti Intan Subadra[1], Arif Hidayat[1], Nandang Mufti[1], Nurul Hidayat[1], Sunaryono[1], Budi Purnama[3], Muhammad Safwan Abd Aziz[4], Ahmad Taufiq[1*]

[1]Department of Physics, Faculty of Mathematics and Natural Sciences, Universitas Negeri Malang, Indonesia
[2]Faculty of Computer Science and Information Technology, Gunadarma University, Indonesia
[3]Department of Physics, Faculty of Mathematics and Natural Sciences, Universitas Sebelas Maret, Indonesia
[3]Department of Physics, Faculty of Sciences, University of Technology Malaysia, Malaysia
*Email: ahmad.taufiq.fmipa@um.ac.id; Tel/Fax: +62-341-552-125

Abstract. This study investigates successfully producing a $Mn_{0.3}Fe_{2.7}O_4$ nanofluid-based magnetic field sensor from iron sand. The characterization exhibited that $Mn_{0.3}Fe_{2.7}O_4$ nanoparticles covered by polyvinyl alcohol (PVA) surfactant were fabricated, as demonstrated by the presence of Fe–O and Mn–O from $Mn_{0.3}Fe_{2.7}O_4$, and C=C, CH_2, C–H, C–C from PVA. A single-phase spinel cubic structure originating from $Mn_{0.3}Fe_{2.7}O_4$ nanoparticles was formed with a crystallite size of 10.5–13.2 nm. Furthermore, based on the scanning electron microscopy image, the nanoparticles had a spherical shape with a particle size distribution of 23.9–33.3 nm. The band gap value increased with PVA surfactant addition from 3.085 eV to 3.504 eV. The $Mn_{0.3}Fe_{2.7}O_4$ nanoparticles with a PVA surfactant had superparamagnetic properties with a saturation magnetization value of 46.45–36.54 emu/g. Furthermore, as the refractive index value of the filler decreased, it affected the application of an optical-based sensor. The light intensity increases close to the magnetic field since only nanofluids near the external source is exposed to the magnetic field. Interestingly, the light intensity after adding PVA was greater than that of the nanofluids without PVA, i.e., up to 2.1 lux. Thus, $Mn_{0.3}Fe_{2.7}O_4$ nanofluids can be potentially applied as a magnetic field sensor.

Keywords: Nanofluid; magnetic field sensor; iron sand; $Mn_{0.3}Fe_{2.7}O_4$; magnetic field

1. Introduction

Today, nanotechnology development has attracted the attention of researchers because of its potential to provide properties superior to those of bulk materials [1]. Technology development is related to the quality of knowledge, which also impacts the daily quality of life [2]. One of the technologies developed by researchers is magnetic sensors. For example, in the communication field, the Internet of Things is used for communication at far distances [3]. Furthermore, magnetic field sensors are also used in navigation technologies such as a compass [4]. In the biomedical field, they detect biological systems used in magnetoencephalography and nuclear magnetic resonance [5]. Many sensors are currently developed based on magnetotransistor, magnetoresistive, fluxgate, or Hall effect [5] – [7]. However, these sensors are still limited as they are expensive, require fabrication conditions in a particular environment at the time of application [9], and require large electricity consumption [9]. Conversely, the magnetic field source also causes pollution and forms electromagnetic interference noise [10].

In the last few years, nanofluid (NF)-based magnetic field sensors have been developed by several researchers [11,12]. NF includes smart materials composed of nanoparticles that function as fillers covered by surfactants and dispersed in a carrier liquid. NF has a magneto-optical effect, including refractive index, tuneability, the Faraday effect, and the magnetochromatic effect [13] – [15], which makes NF a promising magnetic field sensor. In addition, NF has unique properties, especially regarding the flexibility of fluids, which makes it easier to affect

Accepted by Scientia Iranica

particle orientation in response to the external field influence [17]. NF requires a filler with an excellent magnetic response to develop a magnetic field sensor, such as Fe_3O_4 nanoparticles. These nanoparticles have superparamagnetic characteristics with good magnetization saturation and interact well with external magnetic fields [18]. The previous study regarding applying Fe_3O_4 as a magnetic field sensor reported that the laser intensity increases linearly with increasing the external magnetic field [19]. Improving the performance of Fe_3O_4 as a magnetic sensor can be achieved in several ways, such as Mn^{2+} doping. Theoretically, this dopant leads to greater magnetization saturation, where the Mn^{2+} ion has a greater magnetic moment than Fe^{2+} (4 μB), namely 5 μB. According to the calculation, the magnetic moment of $Mn_xFe_{3-x}O_4$ nanoparticles such as $Mn_{0.3}Fe_{2.7}O_4$ increases with the addition of the Mn^{2+} dopant into the Fe_3O_4 system [20]. Moreover, another study confirmed that adding Mn^{2+} dopant increased the saturation magnetization of Fe_3O_4 nanoparticles [19].

Furthermore, the response ability of nanoparticles to a magnetic field depends on the type, shape, and size of nanoparticles. Magnetic materials such as $Mn_{0.3}Fe_{2.7}O_4$ nanoparticles easily aggregate due to van der Waals force, magnetic interactions between particles, and a large surface energy [22]. Aggregation affects and decreases the response to the magnetic field due to the reduced magnetization value. Moreover, aggregation also affects the stability of NF [23], where it causes the structure of the NF to become unstable [24]. Meanwhile, the performance of NF as a magnetic field sensor is good if the stability is high [25]. The aggregation of the NF filler can be minimized by adding a polymer as a template during the synthesis of nanoparticles. Among various existing polymers, polyvinyl alcohol (PVA) is widely chosen as a surfactant because it can produce fillers in dispersed conditions. After all, agglomeration can be prevented, and the PVA coating can prevent the oxidation of magnetite particles [22]. In addition, PVA is composed of hydroxyl groups and a carbon backbone, making PVA hydrophilic. This allows PVA to dissolve in water, resulting in high stability and good chemistry. Furthermore, $Mn_{0.3}Fe_{2.7}O_4$ with a PVA surfactant was coated with a tetramethylammonium hydroxide (TMAOH) as a second surfactant and dispersed in H_2O. TMAOH is a stabilizer that prevents the magnetite nanoparticles in the solution from agglomerating. The combination of $Mn_{0.3}Fe_{2.7}O_4$ with PVA and TMAOH surfactants is expected to have high stability and good magnetic field sensor performance. Based on the literature review, PVA plays an important role in preventing aggregation in $Mn_{0.3}Fe_{2.7}O_4$ nanoparticles. However, the optimal composition of PVA volume to obtain $Mn_{0.3}Fe_{2.7}O_4$ nanofluids with high stability is not reported. Therefore, the role of PVA volume variation is important to investigate in order to produce nanofluids with excellent performance as magnetic field sensors. Furthermore, the research was also carried out to investigate the effect of PVA volume on the structure, morphology, magnetic, and optical properties of $Mn_{0.3}Fe_{2.7}O_4$ NF with double surfactant.

Accepted by Scientia Iranica

2. Experimental Section

2.1. Synthesis of $Mn_{0.3}Fe_{2.7}O_4$ nanofluid with PVA surfactant

In this study, iron sand was used as the primary material for synthesizing $Mn_{0.3}Fe_{2.7}O_4$. $MnCl_2.4H_2O$, hydrochloric acid (HCl), ammonium hydroxide (NH_4OH), PVA, and TMAH were obtained from Merck, and distilled water pro analysis was used. The $Mn_{0.3}Fe_{2.7}O_4$ nanoparticles with PVA surfactant were synthesized using the coprecipitation method. The first step involved preparing a PVA solution by dissolving 2 g of PVA powder in 100 mL of deionized water. Then, the preparation of $FeCl_2$ and $FeCl_3$ solutions was conducted from iron sand [27]. Furthermore, 18 mL of the obtained $FeCl_2$ and $FeCl_3$ solutions were added to $MnCl_2.4H_2O$ and stirred using a magnetic stirrer for 15 min. Then, the solution was titrated with PVA volume variations of 0, 2, 4, 6, 8, and 10 mL, stirred for 30 min, followed by titration of NH_4OH as much as 25 mL for 30 min. After titration, a precipitate of $Mn_{0.3}Fe_{2.7}O_4$ nanoparticles with PVA surfactants was formed. Then, the precipitate was washed with H_2O until the pH was neutral, and 1 g was taken to manufacture NF following the research we had reported previously [12]. The $Mn_{0.3}Fe_{2.7}O_4$ precipitate with the PVA surfactant was dissolved in 2 mL of TMAOH and stirred for 1 h at room temperature. Next, the mixture was dispersed in H_2O and stirred for 1 h at 650 rpm at room temperature. Then, the $Mn_{0.3}Fe_{2.7}O_4$ precipitate with PVA surfactant was dried at 100°C to obtain powder $Mn_{0.3}Fe_{2.7}O_4$ with PVA surfactant. $Mn_{0.3}Fe_{2.7}O_4$ with PVA were then assigned codes P1, P2, P3, P4, P5, and P6, corresponding to Mn0.3Fe2.7O4 with PVA at 0, 2, 4, 6, 8, and 10 mL.

2.2. Characterization

Phase analysis was performed using X-ray diffraction (XRD) type X'Pert Pro to determine the quality of the synthesized $Mn_{0.3}Fe_{2.7}O_4$ NF. XRD characterization was performed to determine the nanoparticle's phase, structure, and crystallite size. Furthermore, the functional groups that make up the nanoparticles were found using Fourier-transform infrared spectroscopy (FTIR), the Shimadzu IR-Prestige 21. In addition, magnetic and optical properties were characterized using a vibrating sample magnetometer (VSM) with the Physical Properties Measurement System Quantum Design PPMS® brand of VersaLab™ Cryogen-free 3 Tesla and UV-Vis Specord 200 Plus, respectively. The performance of NF as a magnetic field sensor was analyzed using an external magnetic field, a laser, and a lux meter. $Mn_{0.3}Fe_{2.7}O_4$NF was placed into a container, then externally magnetized on both sides. Furthermore, the container containing the NF was irradiated by a laser to determine the intensity of the light produced by the sample, where the circuit magnetic sensor testing followed our previous research [28].

Accepted by Scientia Iranica

3. Results and Discussion

3.1. Structure Analysis of $Mn_{0.3}Fe_{2.7}O_4$ with PVA surfactants

The XRD patterns of $Mn_{0.3}Fe_{2.7}O_4$ nanoparticles with a PVA surfactant as an NF filler are shown in Fig 1. Based on the patterns, it was found that all samples had a peak with the same diffraction, which was detected at 2θ values of approximately 30.10^0, 35.50^0, 43.11^0, 56.90^0, and 62.41^0. The diffraction pattern of P1, a pure $Mn_{0.3}Fe_{2.7}O_4$ sample, resembles the peak diffraction of Fe_3O_4 in our previous studies, with the highest peak at 35.65^0 [29]. In comparison, the peaks shifted toward the smaller 2θ. The shift occurred because Mn, with a radius of 0.82 Å, managed to enter the system and replace some Fe ions with a lower radius, 0.77 (Fe^{2+}) and 0.65 (Fe^{3+}). Besides that, the addition of Mn does not create new peaks, such as the usual MnO at 2θ values of 37° (400) and 64.5° (002) [26] . The absence of a new phase was also due to Mn successfully entering the Fe_3O_4 system. Next, peak diffraction after the addition of PVA (P2–P6) showed no difference from the peak of P1. These results confirm that PVA successfully acts as a surfactant. However, the addition of PVA affected the intensity of the peak of $Mn_{0.3}Fe_{2.7}O_4$, where the increase in intensity shows the growth of crystals. This is because PVA contains hydroxyl groups capable of forming hydrogen bonds with anions, which causes the solubility of the metal salt to increase crystal growth [31]. Moreover, the PVA polymer can inhibit cation mobility and prevent $MnFe_2O_4$ decomposition, so forming a new phase can be avoided [28] .

Furthermore, the color lines in Fig. 1 show the diffraction pattern from the fitting results using the AMCSD database model (No. 0007394). The results of the analysis show that peak diffraction represents planes of (2 2 0), (3 1 1), (4 0 0), (3 3 3), and (4 4 0), with the highest peaks being for (3 1 1) at 35.50^0, in accordance with the literature [33]. Furthermore, based on Table 1, it is known that the lattice parameter values ($a = b = c$) of $Mn_{0.3}Fe_{2.7}O_4$ with PVA surfactants are in the range of 8.383 – 8.385 Å. These values were much larger than the lattice parameter value of Fe_3O_4 from previous studies, which range from 8.358 Å to 8.361 Å [27,29]. The increase in the lattice parameter value indicates the presence of Mn^{2+} in the tetrahedral section, indicating that Mn^{2+} successfully replaced some of the Fe^{3+} atoms in the tetrahedral section. It is known that Mn^{2+} has an ionic radius of0.89Å, while the ionic radius of Fe^{3+} = 0.64Å and Fe^{2+} = 0.77Å.

The presence of Mn doping on the tetrahedral site of Fe_3O_4 is in accordance with the Mössbauer results, which are characterized by an increase in the lattice parameter value with the addition of Mn doping. Therefore, the ion distribution of $Mn_{0.3}Fe_{2.7}O_4$ is shown by Equation 1.

Accepted by Scientia Iranica

$$(Mn_x^{2+}Fe_{x-1}^{3+})_{tetra}(Fe_{x-1}^{2+}Fe_{x+1}^{3+})_{octa} \quad (1)$$

In addition, the fitting results confirm that the nanoparticles had a single phase with a cubic spinel structure and a space group of Fd-3m same as Fe_3O_4, as illustrated in Fig. 2. Figure 2 (a) is the structure of Fe_3O_4 which consists of Fe (red sphere) surrounded by six oxygen atoms (blue sphere) or called octahedral site and Fe (orange sphere) which binds four oxygen atoms or often called tetrahedral site. Meanwhile, after Mn doping, it can be seen that in the tetrahedral site, some of the Fe, indicated by the orange sphere, is replaced by a gray sphere, which represents Mn.

Based on Table 1, the lattice parameters of $Mn_{0.3}Fe_{2.7}O_4$ with PVA surfactants were constant, about 8.38 Å. This is consistent with the results of a previous study on the lattice parameters of manganese ferrite particles with the addition of PVA [34]. Furthermore, the crystal sizes obtained ranged from 12.5 ± 1.9 nm to 10.5 ± 1.9 nm. This is due to the effect of adding PVA, where the distortion of bonds between the distance between atoms and compounds is wider, reducing the crystal size [35]. Changes in crystallite size in the sample indicate the successful effect of adding PVA on particle size and retaining the octahedral morphology of samples, where it showed the ability to control particle design [32].

3.2. Functional Groups Analysis of $Mn_{0.3}Fe_{2.7}O_4$ with PVA surfactants

The functional groups of the $Mn_{0.3}Fe_{2.7}O_4$ with PVA surfactant are represented in Fig. 3. Octahedral Fe–O was detected at a wavenumber of 657 cm^{-1}, one of the characteristics of the $Mn_{0.3}Fe_{2.7}O_4$ sample with a PVA surfactant [37,38]. Then, the Mn–O bonds overlapped with Fe–O at a wavenumber of 400–450 cm^{-1}, which shows the displacement of the Mn bonds with Fe in the tetrahedral section [35, 36]. Then, the presence of PVA was confirmed due to the presence of the C=C bond at 1350 cm^{-1}, CH_2 at 856 cm^{-1} [41], C–H at 1502 cm^{-1}, C–C at 1434 cm^{-1}, and O–H at 1639 cm^{-1} [38,12]. Interestingly, with increasing the PVA volume as a surfactant, for $Mn_{0.3}Fe_{2.7}O_4$, OH absorption at 1639 cm^{-1} was widened, a characteristic hydroxyl group of PVA. This indicates that the existing hydroxyl group of PVA increased in the samples along with the increase in the PVA volume. Apart from the functional groups of $Mn_{0.3}Fe_{2.7}O_4$ and PVA, the CO_2 bonds originating from the atmosphere were found at 2380 cm^{-1} [40], and the O–H bond was at 3429 cm^{-1}, which is characteristic of O–H bonds originating from water [34,44,45].

3.3. Morphology of $Mn_{0.3}Fe_{2.7}O_4$ with PVA Surfactants

The morphology of $Mn_{0.3}Fe_{2.7}O_4$ with PVA surfactant was characterized using SEM, and the results are shown in Fig. 4. Overall, the nanoparticles were inclined-shaped spherical with a nearly uniform particle size distribution and uniform agglomeration. Agglomeration occurred because of the ratio between the surface area and the large

Accepted by Scientia Iranica

particle volume, where magnetic dipole interactions and van der Waals forces could stimulate particle agglomeration. Thus, they blocked the formation of a single domain, resulting in inhomogeneity [33]. However, with increasing the PVA volume, the agglomeration of inclined nanoparticles decreased. In addition, the composition of the PVA caused a slowdown in the process. Particle agglomeration and particle homogeneity could be maintained, causing nanoparticles to form more spherical shapes. Based on the quantitative analysis, the particle size distribution ranged from 33.31 ± 0.63 nm to 23.95 ± 0.14 nm, which is close to the results reported previously [41]. The particle size distribution trend of the nanocomposites was consistent with the XRD analysis results. However, it had a value that tended to be greater due to SEM characterization was performed on the sample surface.

3.4. Magnetic Properties of $Mn_{0.3}Fe_{2.7}O_4$ with PVA Surfactants

The magnetic properties of the nanoparticles were characterized using VSM and analyzed using the Langevin method concerning susceptibility. The results of the characterization and analysis are shown in Fig. 5. All samples displayed S-shaped curves, indicating that all $Mn_{0.3}Fe_{2.7}O_4$ with PVA surfactants were superparamagnetic. This is also confirmed by the coercivity and magnetization field remanence values in Table 2, where the value is close to zero, and it can be ignored. The main part of the nanoparticles was superparamagnetic. Furthermore, the magnetization saturation of the nanoparticles ranged from 36.539 ± 0.004 to 46.447 ± 0.056 emu/g. The magnetization saturation value increased and decreased according to the crystal size trend from the XRD analysis. The highest saturation magnetization value was observed in sample P3, which was 46.447 ± 0.056 emu/g, while the lowest saturation magnetization value was obtained in sample P6, which was 36.539 ± 0.041 emu/g. This shows that magnetization saturation in the sample was influenced by the crystal size of the $Mn_{0.3}Fe_{2.7}O_4$ with the PVA surfactant. Based on Table 1, it is known that P3 has the largest crystallite size of 13.4 ± 2.6 nm, while P6 has the smallest crystallite size of 10.5 ± 1.9 nm. In accordance with these results, it can be said that the magnetization value decreases as the crystallite size of $Mn_{0.3}Fe_{2.7}O_4$ with the PVA surfactant decreases. This is confirmed by previous research, where superparamagnetic nanoparticles with a single domain have saturation magnetization values that are directly proportional to size [46]. The decrease in saturation magnetization value in nanoparticles with smaller sizes is due to the fact that small nanoparticles have a large surface area ratio, so that the spin moments on the surface tend to have random orientations. This random orientation is caused by the exchange interaction that keeps the spins parallel, decreasing due to the number of neighbouring atoms surrounding them being fewer than the spin moments in the core. Random surface spins form subdomains

Accepted by Scientia Iranica

containing parallel spins but with different orientations in other subdomains, reducing the total spin alignment and resulting in low magnetization values.

$$\frac{M_{S6} - M_{S1}}{M_{S6}} \times 100\% \quad (2)$$

Based on Table 1, it is known that P6 has a saturation magnetization value of 36.539 ± 0.041 emu/g, which is significantly lower than sample P1, a $Mn_{0.3}Fe_{2.7}O_4$ sample without PVA, with a value of 43.761 ± 0.048 emu/g. According to Equation 2, it can be seen that PVA can affect magnetic intensity by 16.5%. Furthermore, from the saturation magnetization value, an approximation can also be made to determine the effect of PVA on the stability of $Mn_{0.3}Fe_{2.7}O_4$. The colloidal stability of magnetic nanoparticles is influenced by dipolar interactions between particles, which are modeled using dipolar interaction energy (Equations 3 – 5).

$$E_{dip} \approx \frac{\mu_0 \mu^2}{4\pi d^3} \quad (3)$$

If,

$$\mu \approx M_s \times V \quad (4)$$

$$Stabillity \approx \left(\frac{M_{st}}{M_{si}}\right)^2 \quad (5)$$

Then the increase in stability can be calculated by Equation 5, where M_{st} is the saturation magnetization of the last sample and *Msi* is the saturation magnetization of the first sample. In the calculation, the saturation magnetization value of samples P1 and P6 is used. The calculation results show that the stability after the addition of PVA increases to 1.43 times, indicating that the nanofluids are more stable after the addition of PVA.

3.5. Optical Properties of $Mn_{0.3}Fe_{2.7}O_4$ with PVA Surfactants

Fig. 6 shows the direct band gap calculated using Tauc's method. The gap energy of P1, sample $Mn_{0.3}Fe_{2.7}O_4$, was 3.085 eV. The energy gap was similar to that in the previous study, where the resulting energy gap was around 3.01 eV [47]. A previous study reported that the band gap of Fe_3O_4 is 2.3 eV, which is significantly lower than that of sample P1. Mn can increase impurities in semiconductor materials to increase the band gap [48]. This is in line with previous studies where the band gap value of the Fe_3O_4 increased with the addition of other materials and the doping process, ranging from 0 to 4 eV [49]. Furthermore, after adding the PVA surfactant, P2, the band gap value increased by 3.301 eV. This increase is due to the addition of PVA, allowing the material to become more insulating and enhancing the band gap value. Detailed band gap values for the $Mn_{0.3}Fe_{2.7}O_4$ are presented in Table 2. The band gap values after the addition of PVA appear to fluctuate but are larger than that of P1. This may also be related to the particle size, where the band gap value is inversely proportional to the particle size [50].

Accepted by Scientia Iranica

Apart from the band gap, Table 2 shows the refractive index value of $Mn_{0.3}Fe_{2.7}O_4$ with a PVA surfactant. The refractive index is related to the ability of light to propagate or penetrate a substance. The refractive index value plays an important role in the development of optical-based technology, especially optical-based magnetic sensors. The refractive index value is related to the intensity of the laser that can penetrate the NF. The highest refractive index value is shown in sample P1, which is 2.135. This result is in line with previous research, which reported a refractive index of 2.2 [51]. Meanwhile, after the addition of PVA, the refractive index value of the sample tends to be lower than that of P1. This can be attributed to the lower density of the nanoparticles after the addition of PVA (Table 1). Furthermore, the trend of the refractive index value was inversely proportional to the band gap value, where the smaller the band gap value, the larger the refractive index value.

3.6. Sensor Performance of $Mn_{0.3}Fe_{2.7}O_4$ NF with PVA

The sensor performance of $Mn_{0.3}Fe_{2.7}O_4$ NF with PVA surfactant was investigated according to the influence of laser light with a magnetic field applied to the NF. Fig. 7 represents the resulting transmission optics curve, which gives an external magnetic field at a determined distance. This optical transmission occurs because the laser light is passed through the $Mn_{0.3}Fe_{2.7}O_4$ NF in a glass beaker, where the $Mn_{0.3}Fe_{2.7}O_4$ NF generally has isotropic properties, i.e., uniform in all directions, and can absorb only a small amount of laser light when the intensity is high [52].

In this study, the $Mn_{0.3}Fe_{2.7}O_4$ NF samples were diluted using H_2O at a ratio of 1:2. Then, we tested them using a magnetic field in the range of 0–82.5 mT with external magnetic distances of 3, 2.5, 2, 1.5, 1, and 0.5 cm. A greater magnetic field was detected by decreasing the distance. The light intensity enhancement along the magnetic field distance increased near the magnitude of the magnetic field applied to the NF, thereby increasing the ability to absorb laser light. In pure $Mn_{0.3}Fe_{2.7}O_4$ NF without PVA, the obtained light intensity was 0.5 lux; along with the increase in PVA surfactant, the light intensity increased but then decreased. The highest light intensity was observed in sample P4. This is because the P4 sample has a lower refractive index value than the others, namely 1.876 (Table 2). Therefore, the laser will easily penetrate the NF liquid from P4. It is known that the refractive index value is a reflection of the optical density of a liquid, where the smaller the refractive index value, the lower the optical density of the liquid and the laser will more easily penetrate the liquid. Additionally, the decrease in refractive index can also be attributed to polarizability. Previous research has demonstrated a linear relationship between the refractive index value and the polarizability value [53]. PVA is included in the low-polarizability materials because it has –OH functional groups that are not easily polarized. The more PVA solution is added, the more –OH functional groups cover the $Mn_{0.3}Fe_{2.7}O_4$ particles, which restrains electron mobility on

Accepted by Scientia Iranica

the surface and decreases the polarizability of $Mn_{0.3}Fe_{2.7}O_4$, ultimately impacting the decrease in the refractive index value. The smaller the density of a substance will allow light entering the fluid to continue straight away. This phenomenon is explained by the Kerr effect, in which the laser light intensity under the influence of an external magnetic field has a nonlinear effect on the refractive index [54]. Previous studies have stated that the relationship between the laser light intensity, which increases linearly as a function of the external magnetic field, has excellent potential as an optical-based magnetic field sensor. Thus, the study results of $Mn_{0.3}Fe_{2.7}O_4$ NF-based magnetic field sensors have great potential for further development with improvements in various aspects.

4. Conclusion

$Mn_{0.3}Fe_{2.7}O_4$ NF with the PVA surfactant was successfully synthesized. The $Mn_{0.3}Fe_{2.7}O_4$ filler with the PVA surfactant had a cubic spinel structure with lattice parameters of 8.383–8.385 Å. The addition of PVA surfactants did not affect the phase and structure of the nanoparticles; however, the effect on the intensity peak increased. It was noticeable that the growth of the crystals of the nanoparticles was improved. FTIR analysis showed that the main functional groups were Fe–O octahedral and Mn–O and Fe–O tetrahedral at wavenumbers of 657 and 400–450 cm^{-1}, confirming the presence of $Mn_{0.3}Fe_{2.7}O_4$. The presence of PVA was indicated by the presence of C=C at 1350 cm^{-1}, CH_2 at 856 cm^{-1}, and C–H at 1502 cm^{-1}, C–C at 1434 cm^{-1}, as well as the O–H bond at 1639 cm^{-1}. All samples had superparamagnetic properties with magnetization saturation of 46.447–36.539 emu/g. The band gap value of the $Mn_{0.3}Fe_{2.7}O_4$ filler increased with the addition of the PVA surfactant, reaching 3.085–3.504 eV. Furthermore, as the band gap increased, the refractive index decreased, which is very influential for optical-based sensor applications. The performance of $Mn_{0.3}Fe_{2.7}O_4$ NF with PVA surfactant as a magnetic field sensor was indicated by the magnetic field curve against light intensity, where the light intensity increased at closer distances between the magnetic field and the NF. This shows that the magnitude of the external magnetic field that hit the NF was larger at a closer distance. Furthermore, light intensity after adding PVA was greater than that of NF without PVA, i.e., up to 2.1 lux. Based on these results, $Mn_{0.3}Fe_{2.7}O_4$ NF with a PVA surfactant can be applied as a magnetic sensor.

Accepted by Scientia Iranica

Delianti: Writing - original draft, Data curation; ST. Ulfawanti Intan Subadra: Formal analysis, Software; Arif Hidayat: Conceptualization, Writing - original draft; Nandang Mufti: Formal analysis, Resources; Nurul Hidayat: Validation, Resources Sunaryono: Methodology, Resources; Budi Purnama: Data curation, Formal analysis; Muhammad Safwan Abd Aziz: Methodology, Resources; Ahmad Taufiq: Supervision, Project administration, Writing - review & editing

Accepted by Scientia Iranica

Srinivasan, S. and Rajavel, N., "Technology Improves the Quality of Life for Elderly People":, In

et. al., "Self-healable printed magnetic field sensors using alternating magnetic fields", *Nat. Commun.*,

e
t
t
et. al., "Integrated Fluxgate Magnetometer for Use in Isolated Current Sensing", *IEEE J. Solid-State*

7. Langfelder, G. and Tocchio, A., "Operation of Lorentz-Force MEMS Magnetometers With a Frequency

)., "Quantum sensors for biomedical applications", *Nat. Rev. Phys.*, **5**(3), pp. 157–169 (2023).

ct. al., "A giant magnetoresistance sensor for high magnetic field measurements", *Appl. Phys. Lett.*, **77**(12),

p
pt.al., "Ultrasensitive Magnetic Field Sensors for Biomedical Applications", *Sensors*, **20**(6), p. 1569

M
et. al., "Rapid and sensitive magnetic field sensor based on photonic crystal fiber with magnetic fluid

g Ripka, P. and Janosek, M., "Advances in Magnetic Field Sensors", *IEEE Sens. J.*, **10**(6), pp. 1108–1116

f
6
0
et. al., "Fabrication of $Mn_{1-x}Zn_xFe_2O_4$ ferrofluids from natural sand for magnetic sensors and radar

14. Hong, Synthesis of $MnFe_2O_4$/PVA ferrofluid and its application as magnetic sensor, *AIP Conf. Proc.*, AIP,

M
s
16. Martinez, L., Cecelja, F., and Rakowski, R., "A novel magneto-optic ferrofluid material for sensor

pt. al., "Studies on Nanostructure and Magnetic Behaviors of Mn-Doped Black Iron Oxide Magnetic Fluids Synthesized from Iron Sand", *Nano*, **12**(9), pp. 1–11 (2017). https://doi.org/10.1142/S1793292017501107

t. al., "The effect of silica mass ratio on pore structure and magnetic characteristics of Fe_3O_4@SiO_2 core-shell nanoparticles", *Sci. Iran.*, **0**(0), pp. 0–0 (2024). https://doi.org/10.24200/sci.2024.61855.7524

n
et. al., "Studies on Nanostructure and Magnetic Behaviors of Mn-Doped Black Iron Oxide Magnetic Fluids

21. Rhebha Anandhi, J., Antilen Jacob, G., and Justin Joseyphus, R., "Factors affecting the heating efficiency

et. al., “Graphene oxide-Fe_3O_4 nanocomposites as high-performance antifungal agents against Plasmopara v Ivanov, A. S., “On the Reasons for Reversible Aggregation of Magnetite Ferrofluids during Their Dilution with a Pure Carrier in Zero Magnetic Field”, *Colloid J.*, **84**(6), pp. 696–703 (2022). t i
et. al., “Stabilization challenges and aggregation in protein-based therapeutics in the pharmaceutical
25. industry”, *RSC Adv.*, **13**(51), pp. 35987–36006 (2023). https://doi.org/10.1039/D3RA06476J Preparation and S
26. Kim, S. Y., Ramaraj, B., and Yoon, K. R., “Preparation and characterization of polyvinyl alcohol-grafted a b 3
28. Hidayat, A., Taufiq, A., Aturrofi’ah, et. al., “Sensor Performance and Structural Characteristics of C t p F p
et. al., “Low-cost flexible supercapacitors with high-energy density based on nanostructured MnO_2 and
31. Rezaei, M., Mirkazemi, S. M., and Alamolhoda, S., “The Role of PVA Surfactant on Magnetic Properties al., “Exploring the role of Mn^{2+} in the structure, magnetic properties, and radar absorption performance N S
et. al., “Preparation of MnO nanofibers by novel hydrothermal treatment of manganese acetate/PVA o
et. al., “Antibacterial performance of Fe_3O_4/PEG-4000 prepared by co-precipitation route”, *IOP Conf. Ser.*
at. al., “Fabrication of New Fe_3O_4/PVA/$(C_6H_7O_6Na)_n$ Nanohybrid Ferrogels for Antibacterial m Bleszynski, M., Reil, M., and Kumosa, M., “Hydroxyl Group Separation Distances in Anti-Freeze C p
et. al., “Co-precipitation synthesis of (Zn-Mn)-co-doped magnetite nanoparticles and their application in
37. Prasad, A. S., “Iron oxide nanoparticles synthesized by controlled bio-precipitation using leaf extract of G
at. al., “Adsorptive removal of toxic dye using Fe3O4–TSC nanocomposite: equilibrium, kinetic, and h
et. al., “The effect of Mn doping on nano structure and magnetic properties of $Mn_xFe_{3-x}O_4$-PEG/PVP/PVA
Yu, B. Y. and Kwak, S.-Y., “Assembly of magnetite nanocrystals into spherical mesoporous aggregates a with a 3-D wormhole-like pore structure”, *J. Mater. Chem.*, **20**(38), pp. 8320–8328 (2010). https://doi.org/10.1039/C0JM01274B
et. al., “Facile synthesis of PVA-$MnFe_2O_4$ nanocomposite: Its magnetic investigation”, *Mater. Res. Bull.*,
42. Riva’I, I., Wulandari, I. O., Sulistyarti, H., et. al., “Ex-Situ Synthesis of Polyvinyl alcohol(PVA)-coated
et. al., “Sol-gel synthesis and characterization of selected transition metal nano-ferrites”, *Medziagotyra*,
et. al., “Fabrication of single phase superparamagnetic iron oxide nanoparticles directly from soil”, *Sci.*
46. Bipadhyay, S., Parekh, K., and Pandey, B., “Influence of crystallite size on the magnetic properties of Fe_3O_4 nanoparticles”, *J. Alloys Compd.*, **678**, pp. 478–485 (2016). https://doi.org/10.1016/j.jallcom.2016.03.279
4
et. al., “Optimalization of Freezing-Thawing Process in Enhancing Magnetic Properties of

Accepted by Scientia Iranica

et. al., "Mn^{2+}-doped Fe_3O_4 nanoparticles: a novel preparation method, structural, magnetic and e
l
et.al., "Effect of structural and thermal disorder on the optical band gap energy of Cr2O3 nanoparticles",
c Mohanraj, K. and Sivakumar, G., "Synthesis of γ-Fe_2O_3, Fe_3O_4 and copper doped Fe_3O_4 nanoparticles
b
y
o

e

53. Jassim, H. H. and Hashim, F. Sh., "Synthesis of (PVA/PEG: ZnO and Co_3O_4) nanocomposites:
C
h Hasanirokh, K. and Naifar, A., "Quantitative analysis on the optical kerr impact and third harmonic generation in beltrami-shaped curved graphene", *Sci. Rep.*, **15**(1), p. 1666 (2025). https://doi.org/10.1038/s41598-025-85303-9

Accepted by Scientia Iranica

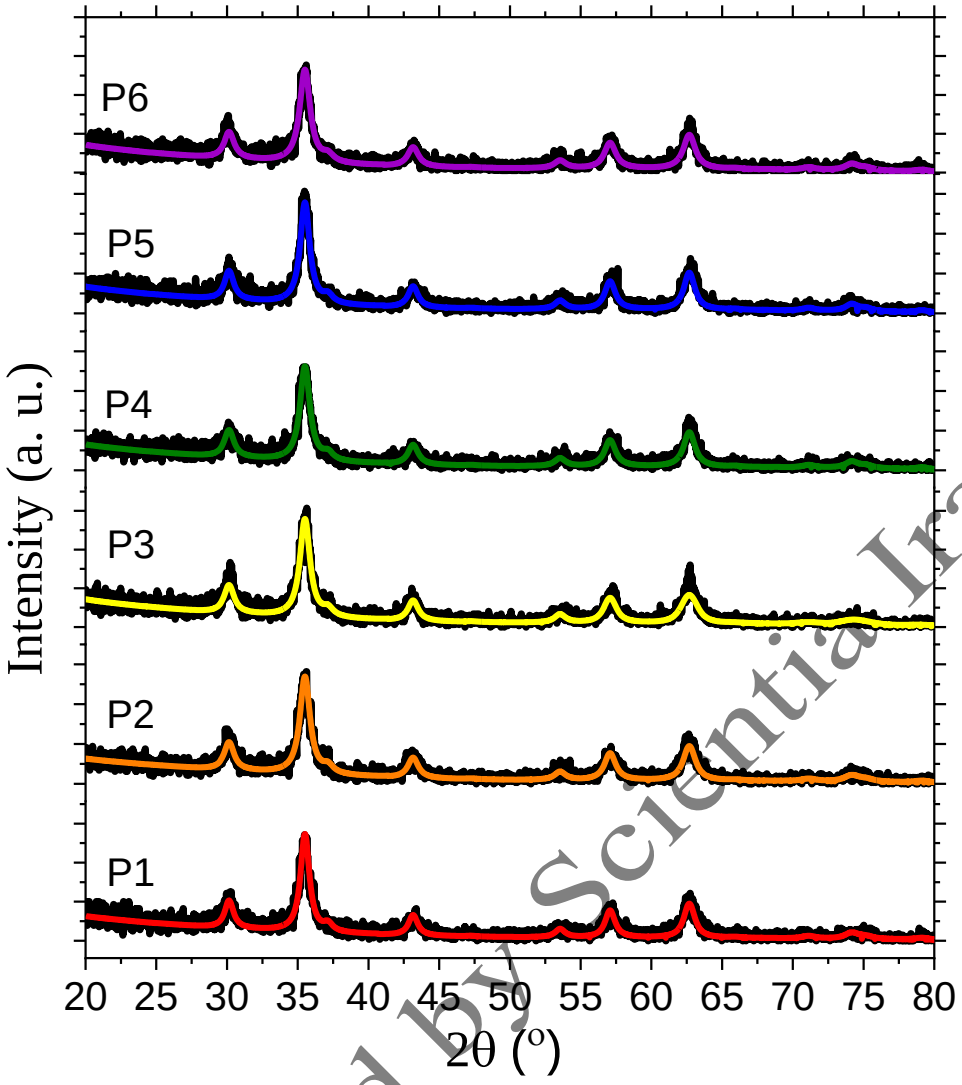

Fig. 1 XRD diffraction patterns of $Mn_{0.3}Fe_{2.7}O_4$ nanoparticles with PVA volume variations

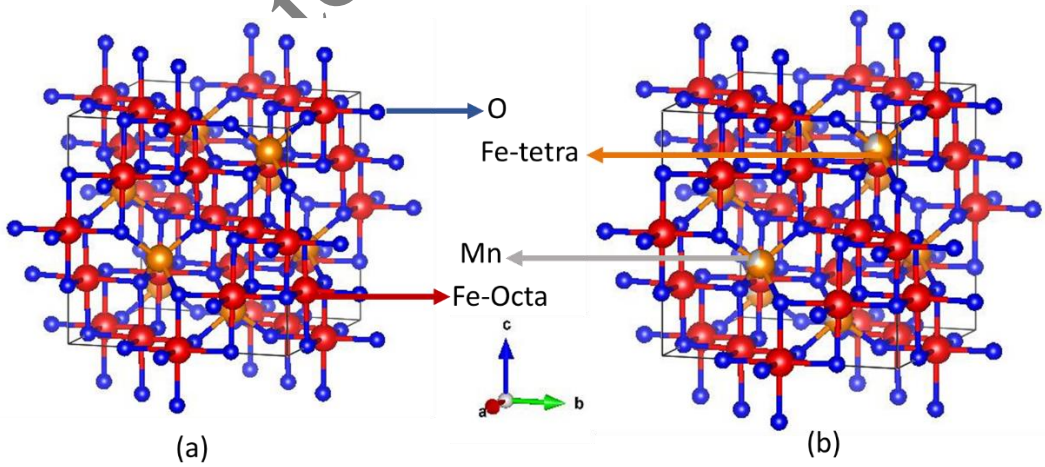

Fig. 2 Crystal structure of (a) Fe_3O_4 and (b) $Mn_{0.3}Fe_{2.7}O_4$

Archive of SID

Scientia Iranica

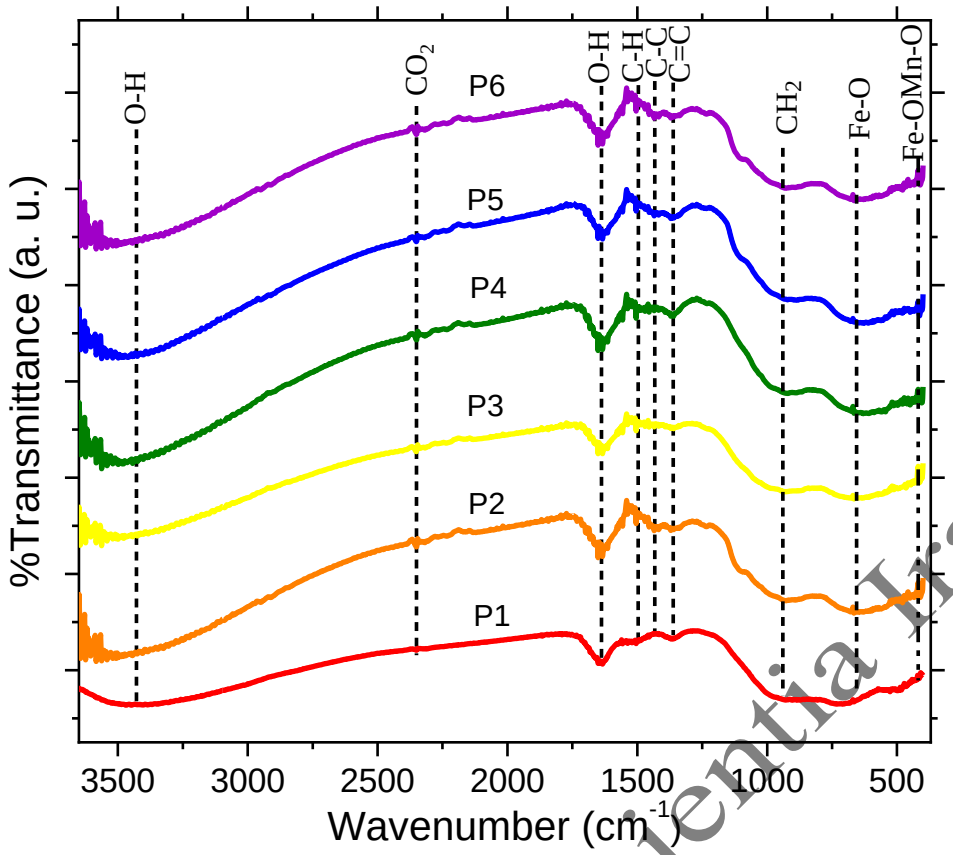

Fig. 3 FTIR spectra of $Mn_{0.3}Fe_{2.7}O_4$ nanoparticles with PVA volume variations

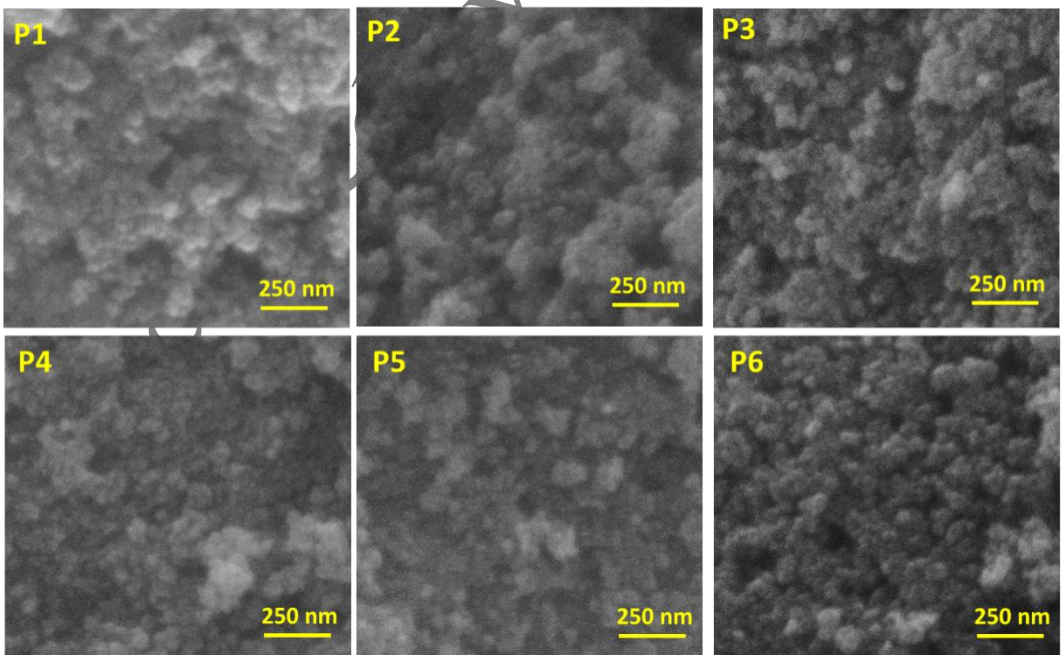

Fig. 4 SEM images of $Mn_{0.3}Fe_{2.7}O_4$ nanoparticles with PVA volume variations

Scientia Iranica

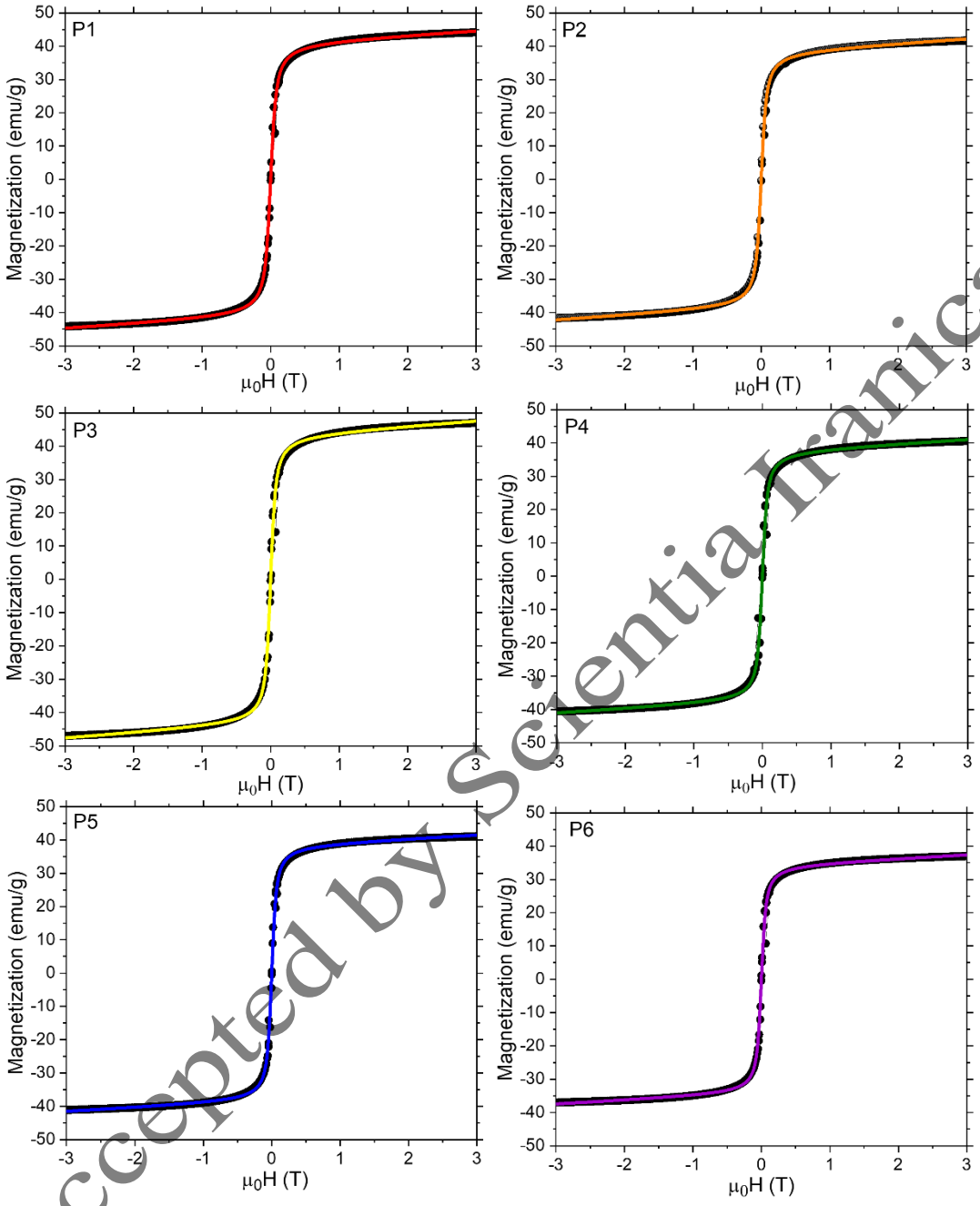

Fig. 5 Hysteresis curves of $Mn_{0.3}Fe_{2.7}O_4$ nanoparticles with PVA volume variations

Accepted by Scientia Iranica

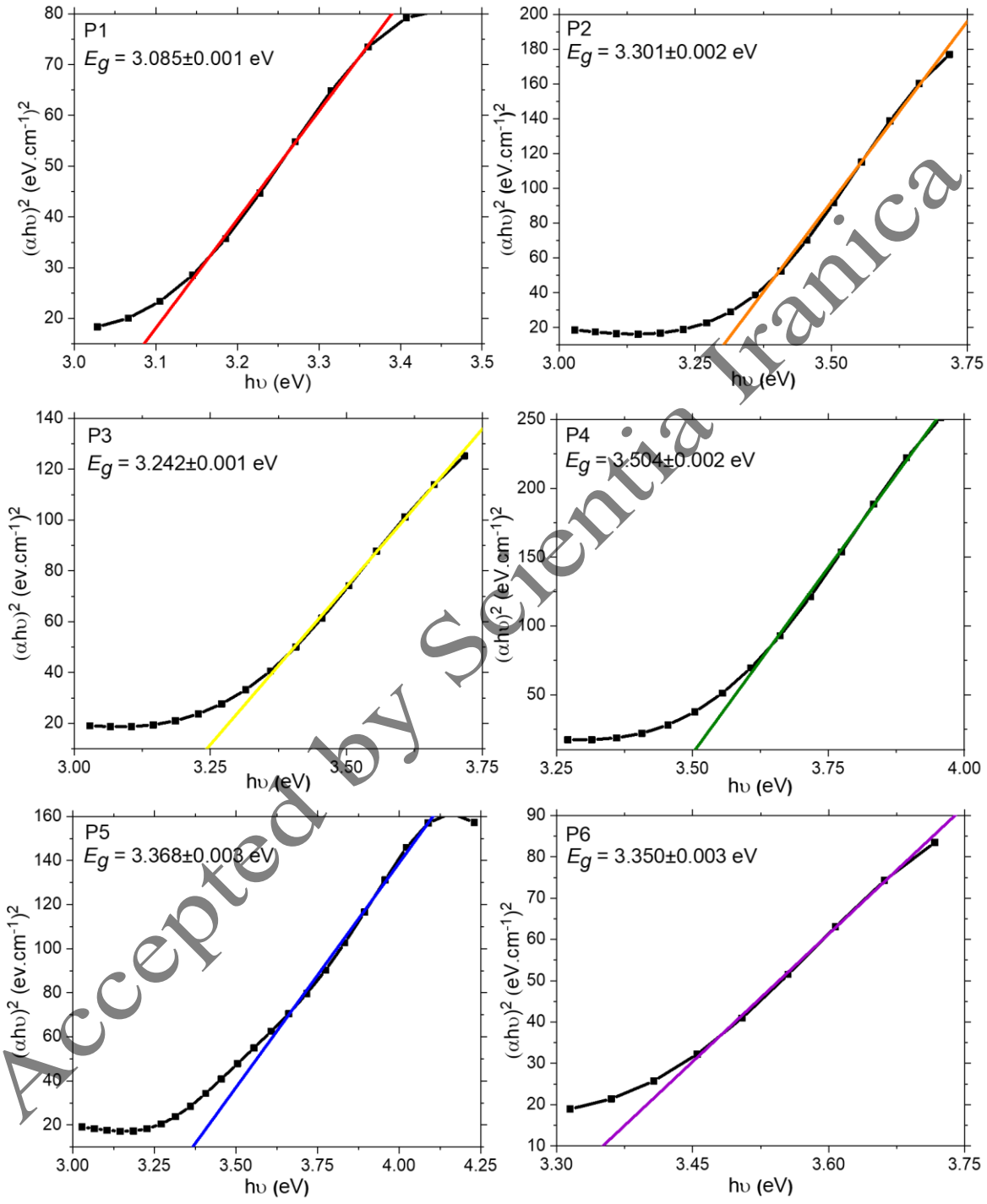

Accepted by Scientia Iranica

Fig. 6 The direct band gap of $Mn_{0.3}Fe_{2.7}O_4$ nanoparticles with PVA volume variations

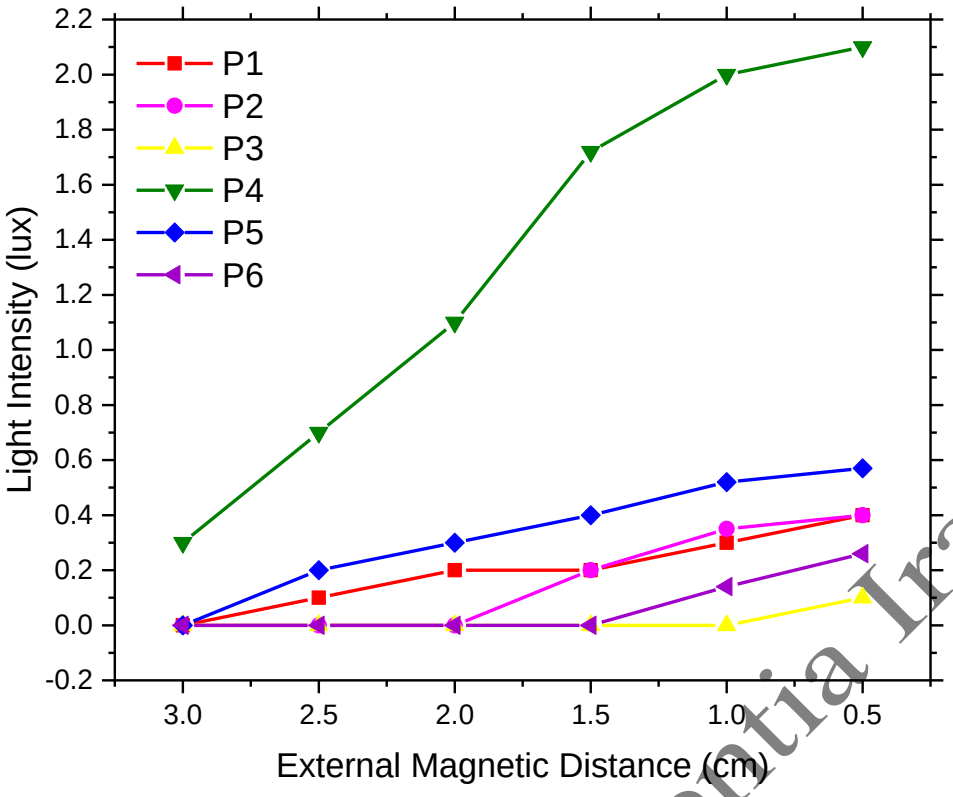

Fig. 7 Sensor performance of $Mn_{0.3}Fe_{2.7}O_4$ NF

Accepted by Scientia Iranica

volume

Samples	$a = b = c$ (Å)	Crystallite size (nm)	Density	Highest peak (^{0})	Bragg R-factor
P1	8.383 ± 0.002	12.5 ± 1.9	5.210	35.50	9.60
P2	8.384 ± 0.001	11.4 ± 1.8	5.189	35.50	8.90
P3	8.383 ± 0.001	13.2 ± 2.6	5.199	35.50	8.60
P4	8.384 ± 0.002	10.9 ± 1.9	5.128	35.50	7.84
P5	8.384 ± 0.001	11.1 ± 2.2	5.147	35.50	8.16
P6	8.385 ± 0.001	10.5 ± 1.9	5.152	35.52	8.52

Table 2 Magnetization saturation value (M_s), magnetization remanence (Mr), field coercivity (Hc), and susceptibility (χ)

Samples	M_s (emu/g)	M_r (emu/g)	H_c (T)	χ
P1	43.761 ± 0.048	0.059 ± 0.030	0.001 ± 0.001	1.273 ± 0.036
P2	41.154 ± 0.046	0.002 ± 0.001	0.002 ± 0.001	1.327 ± 0.029
P3	46.447 ± 0.056	0.038 ± 0.028	0.001 ± 0.000	1.485 ± 0.042
P4	40.067 ± 0.039	0.027 ± 0.002	0.002 ± 0.001	1.239 ± 0.039
P5	40.627 ± 0.032	0.017 ± 0.013	0.003 ± 0.001	1.081 ± 0.026
P6	36.539 ± 0.041	0.038 ± 0.041	0.002 ± 0.001	1.077 ± 0.031

Sample	Band gap (eV)	Refractive index
P1	3.085	2.135
P2	3.301	2.001
P3	3.242	2.038
P4	3.504	1.876
P5	3.368	1.959
P6	3.350	1.971

Accepted by Scientia Iranica

Delianti received her B.S. degree in Physics from Universitas Mulawarman and her master's degree in Physics from Universitas Negeri Malang, Indonesia. Her research interests focus on the fabrication of nanofluids for magnetic field sensors.

ST. Ulfawanti Intan Subadra is a researcher at the AT Research Department of Physics, Universitas Negeri Malang, Indonesia. She received her B.S. degree and master's degree in physics from Universitas Negeri Malang. Her research interests focus on nanomagnetic and its applications in sensors, radar-absorbing materials, and the medical field.

Arif Hidayat received his Ph.D. from Université de Lille, France. He is a Senior Professor at the Department of Physics, Universitas Negeri Malang. He has published more than one hundred scientific articles with research interests in nanofluid, optics, and sensors.

Nandang Mufti achieved his Ph.D. from the University of Groningen, the Nederland. Now, he is a Professor at the Department of Physics and head of the Innovation Directorate at Universitas Negeri Malang. He has many grants and publications related to materials sciences.

Nurul Hidayat is an Associate Professor and Head of Laboratories at the Department of Physics, Universitas Negeri Malang. He earned his Ph.D. from the Universiti Teknologi Malaysia. He has published numerous scientific papers focusing on nanomaterials, nanomagnetic, and optical sensors.

Sunaryono is a Professor at the Department of Physics, Universitas Negeri Malang. He earned his Ph.D. from the Institut Teknologi Sepuluh Nopember, Indonesia. He has numerous research grants and published scientific articles, focusing on nanomagnetic materials.

Budi Purnama is a Professor and head of the Department of Physics, Universitas Sebelas Maret, Indonesia. He develops magnetic materials. He has published over a hundred scientific articles in reputable international journals.

Muhammad Syaifwan Hakim Abdon Azis is a Professor and the Head of the Department of Physics at Universitas Negeri Malang. In 2023,

Accepted by Scientia Iranica